

Strain-mediated electric-field control of photoinduced demagnetization in $\text{La}_{0.8}\text{Ca}_{0.2}\text{MnO}_3$ thin films

E. J. Guo,^{1,2} J. Gao,^{1,a)} and H. B. Lu²

¹Department of Physics, The University of Hong Kong, Pokfulam Road, Hong Kong

²Beijing National Laboratory for Condensed Matter Physics, Institute of Physics, Chinese Academy of Sciences, Beijing 100190, People's Republic of China

(Received 24 September 2010; accepted 29 January 2011; published online 22 February 2011)

$\text{La}_{0.8}\text{Ca}_{0.2}\text{MnO}_3$ (LCMO) thin films have been epitaxially grown on ferroelectric $0.67\text{Pb}(\text{Mg}_{1/3}\text{Nb}_{2/3})\text{O}_3$ - 0.33PbTiO_3 (PMN-PT) substrates. The substrate-induced strain effects on the transport and photoinduced demagnetization in LCMO films were investigated. The photoinduced resistances (PRs) of LCMO systematically changed versus temperature before and after ferroelectric-poling on PMN-PT, indicating that photoexcited extra carriers in LCMO may suppress the neighboring spin correlation due to the photoassisted hopping of anti-Jahn–Teller polarons. Moreover, a significant modulation on PR by electric fields applied across PMN-PT was observed. *In situ* x-ray diffraction indicates that the observed variations result from substrate-induced strain due to the ferroelectric polarization or converse piezoelectric effect.

© 2011 American Institute of Physics. [doi:10.1063/1.3556613]

The doped manganites are strongly correlated electron system with charge, orbital, and lattice degrees of freedom; therefore, rich physical phenomena were observed, such as colossal magnetoresistance (CMR),¹ charge/orbital ordering (CO),² and electrical phase separation.³ At the same time, the manganites located on the phase boundary are sensitive to the external field including magnetic field, electrical field, current, and light.^{4–9} Light irradiation, being one of the external perturbations, offers a convenient way to modify the concentration of carriers and induce the changes in the manganites. Among all the photoinduced effects, photoinduced resistance change and demagnetization in the doped manganites are fascinating phenomena which had been extensively studied.^{6–9} Both of them think the injection of a large number of photoexcited e_g carriers, which are expected to significantly affect the magnetic interaction and to modify the t_{2g} -spin ordering, changes the antiferromagnetic/ferromagnetic phase balance in the films, favoring the insulating antiferromagnetic state.

Recently, a number of studies had been focused on how substrate-induced lattice strain, which could change the strength of the double-exchange interaction and Jahn–Teller (JT) electron-lattice coupling via modifying Mn–O bond lengths and/or Mn–O–Mn bond angles, will affect the physical properties of manganite thin films.^{10–15} However, strain effects on the photoinduced effects in the manganites have rarely been reported. In this letter, the substrate-induced strain effects on the transport and the photoinduced demagnetization in LCMO film were carefully studied using an epitaxial $\text{La}_{0.8}\text{Ca}_{0.2}\text{MnO}_3/0.67\text{Pb}(\text{Mg}_{1/3}\text{Nb}_{2/3})\text{O}_3$ - 0.33PbTiO_3 (LCMO/PMN-PT) composite. The modulation of resistance and photoinduced resistance (PR) by the induced lattice strain in the PMN-PT substrates was observed.

The commercial ferroelectric (001)-oriented PMN-PT single crystal was chosen as substrates due to its perovskite-type cubic lattice structure and outstanding ferroelectric po-

larization and converse piezoelectric effects. Therefore, it is a good candidate for investigating the effects of strain-mediated electrical control of physical properties in manganites. In our experiment, the geometry of PMN-PT wafer is $3\text{ mm} \times 3\text{ mm}$ with thickness of 0.5 mm. The LCMO thin film was grown on PMN-PT by pulsed laser deposition using a KrF excimer laser with a wavelength of 248 nm.¹⁶ The pulse frequency was 2 Hz, and the energy of laser beam was $\sim 300\text{ mJ}$. The temperature of the substrate was kept at about $700\text{ }^\circ\text{C}$ and the oxygen pressure was maintained at 0.5 mbar throughout the deposition. The film thickness was $\sim 40\text{ nm}$, controlled by the deposition time. After the deposition, the as grown film was *in situ* annealed in pure oxygen of 1 atm for 30 min. Then, four silver contact pads were prepared on LCMO film by thermal evaporation. Also, the current leads were connected to the silver pads using a MEI-907 supersonic wire bonder to obtain low Ohmic contacts. The light source used in our experiment is a semiconductor laser with wavelength of 532 nm and power density of 3 mW/cm^2 .

The crystallization of the LCMO film was examined by x-ray diffraction (XRD). Figure 1 shows a typical XRD $\theta \sim 2\theta$ spectrum of the LCMO/PMN-PT structure. Besides the reflection of the substrate and the (00 l) diffraction peaks of the LCMO, no other peaks from the impurity phases or randomly oriented grains can be observed, indicating that the film is *c*-axis preferentially oriented. We also measured the rocking curve of the (002) peak of LCMO [shown in the inset of Fig. 1(a)]. It presents a very small value ($\sim 0.3^\circ$) of full width at half maximum, implying a highly epitaxy and good crystallization of LCMO film.

The resistance of the LCMO films was measured using a standard four-probe method in a closed-cycle cryostat, and the schematic of measuring circuit was shown in the inset of Fig. 1(b). An external dc high-voltage source was used to apply an electric-field E across the PMN-PT crystal. LCMO was served as top electrode due to its small resistance ($\sim \text{k}\Omega$) compared with huge resistance of PMN-PT substrate ($\sim \text{G}\Omega$). Figure 2 shows the temperature dependence of the

^{a)}Author to whom correspondence should be addressed. Electronic mail: jugao@hku.hk.

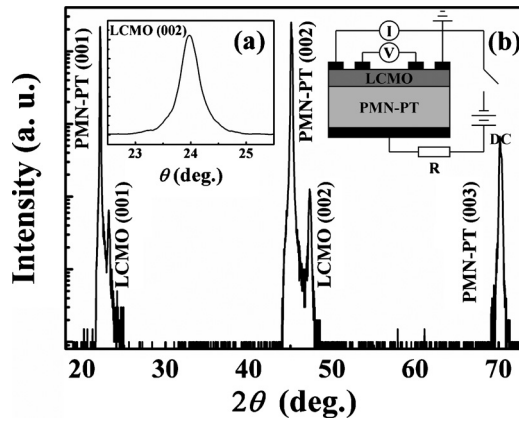


FIG. 1. XRD $\theta \sim 2\theta$ scanning curve of LCMO/PMN-PT structure. The inset (a) shows the rocking curve of LCMO (002) reflection peak. The inset (b) shows the schematic diagram of the LCMO/PMN-PT structure and measurement circuit.

resistance for LCMO film with and without light, respectively. When PMN-PT substrate was in the unpolarized state (referred to as P_r^0), the resistance of LCMO increases with temperature decreasing and undergoes a paramagnetic (PM) insulating state to ferromagnetic (FM) metallic state transition at $T_p \sim 222$ K, exhibiting the typical electrical characteristics of CMR materials. In order to investigate the strain effect induced by ferroelectric polarization to the LCMO layer, we positively polarized the PMN-PT *in situ* at room temperature by applying an electrical field $E = +10$ kV/cm, which is much larger than the coercive field of PMN-PT of ~ 2.8 kV/cm.¹³ Here, the positive direction is defined by the electric dipole moment in the PMN-PT point toward the LCMO. After *in situ* poling for 30 min, we turned off the electric field, and PMN-PT was in the positively polarized state (referred to as P_r^+). As seen in Fig. 2, ferroelectric polarization shifts the T_p slightly to a higher temperature of ~ 223.7 K and the resistance decreases significantly in a wide temperature range. The resistance of LCMO was also measured under the same conditions when LCMO was irradiated by light and the photoinduced demagnetization effect was investigated. The inset of Fig. 2 presents the temperature dependence of photoinduced resistance changes ($PR = R_{\text{light}} - R_{\text{dark}}$) when the PMN-PT was in P_r^0 and P_r^+ states, respectively. The PR in different polarization states showed the same variation. It reached the minimum values of -56Ω for

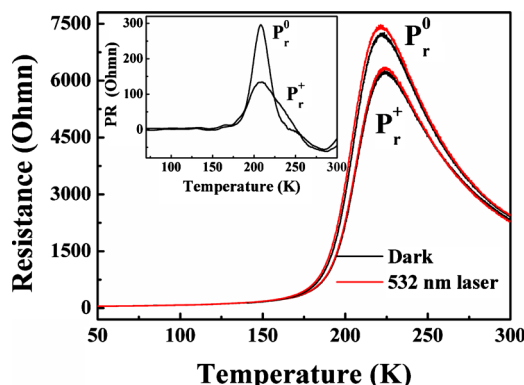


FIG. 2. (Color online) The temperature dependence of resistance for the LCMO film kept in the dark and under the irradiation of 532 nm laser when the PMN-PT substrate is in P_r^0 and P_r^+ states, respectively. The inset shows that the PR changes with temperature when the PMN-PT substrate is in P_r^0 and P_r^+ states.

P_r^0 and -60Ω for P_r^+ at ~ 283 K, and the maximum values of 296Ω for P_r^0 and 135Ω for P_r^+ at ~ 208 K, respectively. Note that the PR was negative when LCMO was in PM insulating state, while it turned out to be positive when LCMO underwent insulator-to-metal transition into FM metallic state. It is known that the transport of doped manganites is closely related to the spin system of e_g carriers and localized t_{2g} spin core in Mn ions. At $T > T_p$, the localized e_g carriers and lattice distortion formed small (anti-JT) polarons, which were formed when holes are doped into LCMO, so the transport of LCMO is small polaron hopping conduction in the PM insulating state. With further decreasing temperature, the double-exchange (DE) effect plays a key role in the transport of LCMO. The e_g electrons of Mn^{3+} ions jump more easily between Mn^{3+} and Mn^{4+} ions through O^{2-} ions and the film forms FM metallic conduction, resulting in a reduction of resistance. The photoenergy of 532 nm laser is about 2.34 eV, which is much larger than the band gap of LCMO ~ 1 eV. In the insulating state, light can excite more photoinduced carriers and enhanced hopping of small polarons, leading to a decrease of the film resistance. On the contrary, in the metallic state, light could excite spin-down e_g electrons, which destroy the FM coupling between spin-up e_g and t_{2g} electrons in Mn^{3+} ions. As a result, it weakens the DE effect and enhances the resistance of LCMO.

To study the strain effect on the transport and the photo-induced demagnetization in LCMO films, we measured the resistance of LCMO versus temperature with and without light by applying different electric-field E to the LCMO/PMN-PT structure when PMN-PT was in P_r^+ state. Figure 3(a) presents that the resistance of LCMO systematically decreases with increasing E from 0 to 10 kV/cm when LCMO was kept in the dark. The relative decrease in the resistance ($\Delta R/R$) under different electric fields is shown in the inset of Fig. 3(a). The $\Delta R/R$ shows a linear dependence on E at both high and low temperatures. When E increases from 0 to 10 kV/cm, the resistance decreased by $\sim 5.63\%$, 7.74% , 10.65% , 18.08% , and 31.06% at different temperatures (270, 250, 230, $T_p \sim 224$, and 210 K), respectively. When LCMO was irradiated by light, the resistance of LCMO exhibits the same variation as that kept in the dark (the results were not shown here). As shown in the inset of Fig. 3(b), we found that T_p increase linearly with increasing E , no matter it is in dark or under light irradiation. Figure 3(b) shows the temperature dependence of PR under different E . It was found that PR was strongly modulated by electric-field E . The maximum values of PR increase from 135 to 477 Ω for E increasing from 0 to 10 kV/cm.

We also polarized the PMN-PT negatively (referred to as P_r^-) and measured the resistance of LCMO varied with applied field E , with and without light. It was found that the resistance of LCMO for P_r^- was almost the same as that for P_r^+ , and the T_p also coincided with that for P_r^+ . The same results had been observed in other doped manganites.¹¹⁻¹³ It was reported that the ferroelectric field effect plays a negligible effect in this situation, since the electronic screening length in the manganite films is much smaller than the thickness of the film. Therefore, ferroelectric polarization induced lattice strain in PMN-PT substrates, which would be transferred to LCMO, is the reason that greatly affects the physical properties of LCMO. To verify this point of view, we measured *in situ* the XRD curves from 44° to 48° by apply-

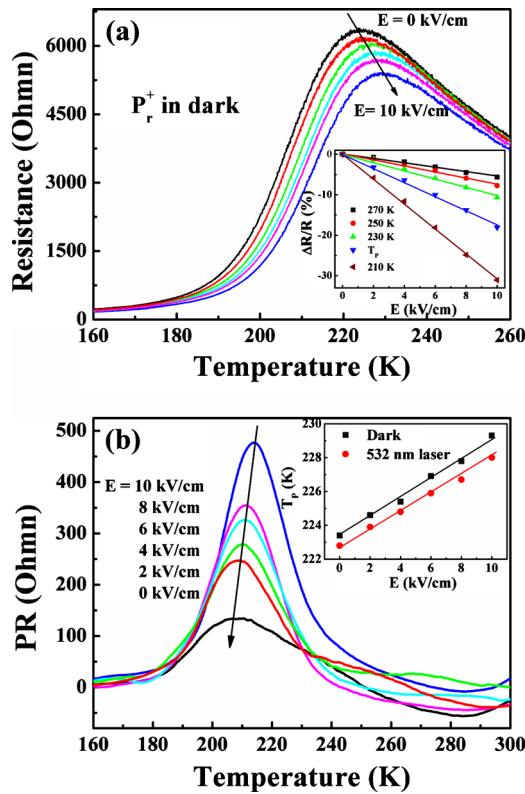


FIG. 3. (Color online) (a) The temperature dependence of resistance for the LCMO film by applying different electric-field E when LCMO is kept in the dark and PMN-PT is in P_r^+ state. The inset shows the relative changes in the resistance of LCMO as a function of applied electric-field E under different measuring temperatures. (b) The temperature dependence of PR for the LCMO film when the different electric-field E is applied to LCMO/PMN-PT structure. The inset shows the T_p as a function of E when LCMO is kept in the dark and under the irradiation of 532 nm laser, respectively.

ing different E to a LCMO/PMN-PT structure at room temperature. It was found that LCMO (002) and PMN-PT (002) reflection peaks systematically shift to the lower 2θ values with increasing E from 0 to 10 kV/cm, as shown in the inset of Figs. 4(a) and 4(b), respectively. The calculated out-of-plane lattice constant c of PMN-PT increases from 4.019 to 4.031 Å and that of LCMO increases from 3.849 to 3.858 Å when E increases from 0 to 10 kV/cm, respectively. Figure 4 shows the linear dependence of relative changes $\Delta c/c$ of

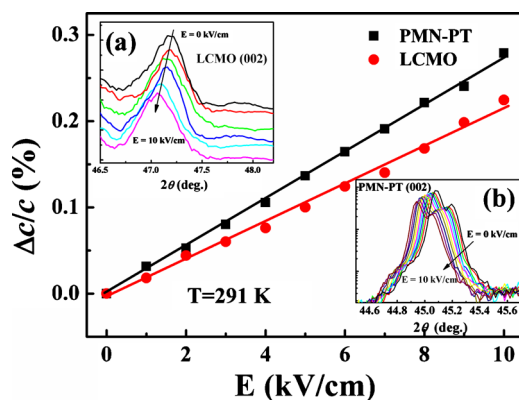


FIG. 4. (Color online) The relative changes in the lattice constants $\Delta c/c$ of the LCMO film and the PMN-PT substrate as a function of electric-field E . Insets (a) and (b) present the *in situ* XRD patterns in the vicinity of (002) reflections for the LCMO film and PMN-PT substrate under different electric fields, respectively.

PMN-PT and LCMO with increasing E , indicating the piezoelectric nature of induced strain in PMN-PT. The maximum values of $\Delta c/c$ for PMN-PT and LCMO were 0.279% and 0.224% when $E=10$ kV/cm, respectively. The out-of-plane compression strain ε_{zz} [defined as $\varepsilon_{zz}=(c_{\text{film}}-c_{\text{bulk}})/c_{\text{bulk}}$] of LCMO is reduced from -0.79% to -0.56% (i.e., $\Delta\varepsilon_{zz}=0.23\%$). Assuming approximate volume preserving distortion, an increase in $\Delta\varepsilon_{zz}$ by 0.23% would be accompanied by a decrease in the in-plane tensile strain $\Delta\varepsilon_{xx}$ of LCMO by 0.115% using the expression $\Delta\varepsilon_{zz}=-2\nu/(1-\nu)\Delta\varepsilon_{xx}$, where $\nu(=0.5)$ is the Poisson ratio. The same results were observed by Thiele *et al.*¹¹ and Zheng *et al.*¹³ It was generally believed that the strain effects on the properties of LCMO are attributed to the reduction of in-plane tensile strain in LCMO, which will influence the JT-type distortion in MnO_6 octahedra and further weaken the electron-lattice coupling. Thus, a higher electric-field E will lead to a much heavy distortion in MnO_6 octahedra, result in a reduction of the separation between upper t_{2g} and lower e_g levels,¹² and the observed larger PR is understandable.

In conclusion, LCMO films were epitaxially grown on PMN-PT crystals and the effects of substrate-induced strain on the transport and photoinduced demagnetization properties of LCMO were investigated. It was found that the resistance and PR strongly depend on the electric field applied on the LCMO/PMN-PT structure, which induced the in-plane tensile strain into the LCMO layer. The *in situ* XRD analysis indicates that the variation of resistance and PR result from the induced strain due to the ferroelectric polarization or the converse piezoelectric effect.

This work has been supported by the Research Grant Council of Hong Kong (Project No. HKU702409P) and the URC of University of Hong Kong.

- ¹R. von Helmolt, J. Wecker, B. Holzapfel, L. Schultz, and K. Samwer, *Phys. Rev. Lett.* **71**, 2331 (1993).
- ²R. Schmidt, *Phys. Rev. B* **77**, 205101 (2008).
- ³A. Biswas, M. Rajeswari, R. C. Srivastava, T. Venkatesan, R. L. Greene, Q. Lu, A. L. de Lozanne, and A. J. Millis, *Phys. Rev. B* **63**, 184424 (2001).
- ⁴J. Gao, S. Q. Shen, T. K. Li, and J. R. Sun, *Appl. Phys. Lett.* **82**, 4732 (2003).
- ⁵N. Takubo, Y. Ogimoto, M. Nakamura, H. Tamaru, M. Izumi, and K. Miyano, *Phys. Rev. Lett.* **95**, 017404 (2005).
- ⁶K. Matsuda, A. Machida, Y. Moritomo, and A. Nakamura, *Phys. Rev. B* **58**, R4203 (1998).
- ⁷Y. G. Zhao, J. J. Li, R. Shreekala, H. D. Drew, C. L. Chen, W. L. Cao, C. H. Lee, M. Rajeswari, S. B. Ogale, R. Ramesh, G. Baskaran, and T. Venkatesan, *Phys. Rev. Lett.* **81**, 1310 (1998).
- ⁸V. Moshnyaga, A. Giske, K. Samwer, E. Mishina, T. Tamura, S. Nakabayashi, A. Belenchuk, O. Shapoval, and L. Kulyuk, *J. Appl. Phys.* **95**, 7360 (2004).
- ⁹H. Huhtinen, R. Laiho, and V. Zakhvalinskii, *Phys. Rev. B* **71**, 132404 (2005).
- ¹⁰W. Eerenstein, M. Wiora, J. L. Prieto, J. F. Scott, and N. D. Mathur, *Nature Mater.* **6**, 348 (2007).
- ¹¹C. Thiele, K. Dörr, S. Fähler, L. Schultz, D. C. Meyer, A. A. Levin, and P. Paufler, *Appl. Phys. Lett.* **87**, 262502 (2005).
- ¹²A. D. Rata, A. Herklotz, K. Nenkov, L. Schultz, and K. Dörr, *Phys. Rev. Lett.* **100**, 076401 (2008).
- ¹³R. K. Zheng, Y. Wang, H. L. W. Chan, C. L. Choy, and H. S. Luo, *Appl. Phys. Lett.* **90**, 152904 (2007).
- ¹⁴Z. G. Sheng, J. Gao, and Y. P. Sun, *Phys. Rev. B* **79**, 174437 (2009).
- ¹⁵R. K. Zheng, Y. Jiang, Y. Wang, H. L. W. Chan, C. L. Choy, and H. S. Luo, *Phys. Rev. B* **79**, 174420 (2009).
- ¹⁶J. Gao and F. X. Hu, *Appl. Phys. Lett.* **86**, 092504 (2005).